# Absolute configuration of chirally deuterated neopentane

J. Haesler[1], I. Schindelholz[1], E. Riguet[1], C. G. Bochet[1] & W. Hug[1]

[1]Department of Chemistry, University of Fribourg, ch. du Musée 9, CH-1700 Fribourg, Switzerland.

**The relationship between macroscopic chirality and chirality on the molecular level was unequivocally established in 1951 through anomalous X-ray scattering[1]. Although this technique became the definitive method for determining the absolute configuration of a molecule, one important limitation of the approach is that the molecule must contain 'heavy' atoms (for example, bromine). The direct determination of absolute configurations for a wider range of molecules has recently become possible by measuring a molecule's vibrational optical activity[2,3]. Here we show that instrumental advances in Raman optical activity[4,5], combined with quantum chemical computations[6–8], make it possible to determine the absolute configuration of (R)-[$^2H_1$, $^2H_2$, $^2H_3$]-neopentane[9]. This saturated hydrocarbon represents the archetype of all molecules that are chiral as a result of a dissymmetric mass distribution. It is chemically inert and cannot be derivatized to yield molecules that would reveal the absolute configuration of the parent compound. Diastereomeric interactions with other molecules, optical rotation, and electronic circular dichroism are, in contrast to the well-known case of bromochlorofluoromethane[10–12], not expected to be measurable. Vibronic effects in the vacuum ultraviolet circular dichroism might reveal that the molecule is chiral, but the presence of nine rotamers would make it extremely difficult to interpret the spectra, because the spatial arrangement of the rotamers' nuclei resembles that of enantiomers. The unequivocal spectroscopic determination of the absolute configuration of (R)-[$^2H_1$, $^2H_2$, $^2H_3$]-neopentane therefore presented a major challenge, one that was at the very limit of what is possible.**

The synthesis of enantioenriched (R)-[$^2H_1$, $^2H_2$, $^2H_3$]-neopentane **1** is itself a challenge. It bears a quaternary chiral centre, the substituents of which are differentiated only by their isotopic pattern; it is gaseous at room temperature and pressure, and it is highly flammable. The intuitive retrosynthetic analysis based on the deprotonation/alkylation of an α-$CD_3$-substituted chiral propionate derivative (see Supplementary Information) fails because the high electronic and steric similarity between the $CH_3$ and the $CD_3$ groups prevent the preferential formation of one of the two diastereomeric enolates.

We therefore decided to exploit the difference in shape between a tetrahedral C$sp^3$ and a trigonal C$sp^2$ carbon by a γ-deprotonation/α-alkylation sequence as shown in Fig. 1 (see Supplementary Information for full protocols and characterization). Hence, treatment of the chiral oxazolidinone derivative **4** with sodium hexamethyldisilazide, followed by alkylation with perdeuterated methyl iodide provided the compound **5** with a diastereomeric purity of 95% (the diastereomeric ratio was measured by hydrogen nuclear magnetic resonance, $^1H$-NMR); its absolute configuration was assigned by analogy to a closely related alkylation[13]. At this point, the chiral quaternary centre bears no risk of racemization, and the optical purity can be assumed to be 95% enantiomeric ratio (e.r.) throughout the rest of the synthesis. Reductive removal of the chiral auxiliary with lithium aluminium deuteride, followed by ozonolysis and *in situ* reduction with sodium borodeuteride, gave the diol **7**, which was then converted into the stable and non-volatile dimesylate **8**. $^1H$-NMR analysis confirmed the expected 1:3 ratio of methylene versus
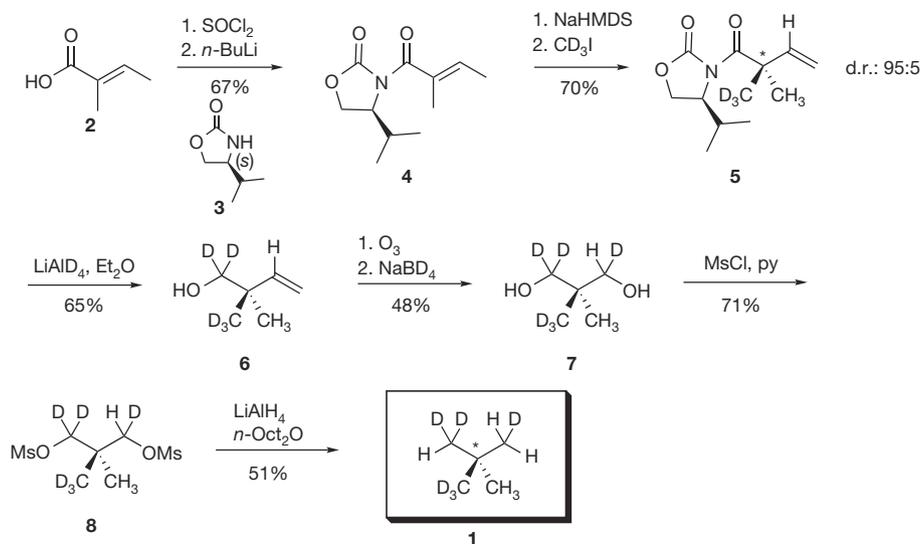


**Figure 1 | Synthetic route to chirally deuterated neopentane 1.** Yields are given in percentage. d.r., diastereomeric ratio. NaHMDS, sodium hexamethyldisilazide; Et$_2$O, diethyl ether; Ms, mesyl; py, pyridine.

methyl resonances, also compatible with the reference mesylate $CH_3$ groups (see Supplementary Information). Displacement of both mesylates was performed by an excess of lithium aluminium hydride at 50 °C in a sealed tube for 48 h. $(R)$-[$^2H_1$, $^2H_2$, $^2H_3$]-neopentane **1** was collected by room pressure and room temperature distillation into a NMR tube precooled to 77 K. The tube was then sealed by fusion.

Owing to the procedure used to collect the sample, the yield (30 mg, 51%) was evaluated spectroscopically by proton NMR with an internal standard (25 mg of **1** were collected in the NMR tube and 5.1 mg in a glass capillary for Raman measurements). $^1$H-NMR shows three distinct resonances at 0.89, 0.87 and 0.86 p.p.m. with the integral ratios (3:2:1) and multiplicity (singlet, triplet and quintet), expected for the peripheral $CH_3$, $CH_2D$ and $CHD_2$ groups (see Supplementary Information). The $^2$H-NMR spectrum shows three broad singlets in the methyl regions. Interestingly, it is in the $^{13}$C-NMR (with $^1$H broadband decoupling) that all the methyl groups are visible, confirmed by the corresponding DEPT-135 sequence (see Fig. 2).

Noise and deterministic spurious signals are the two biggest problems in Raman optical activity. The criterion for its measurability is less the absolute size than the ratio of Raman optical activity (ROA) to Raman scattering, commonly designated by $\varDelta$ (ref. 14). From the computed spectra it was estimated that $\varDelta$ for the mixture of the rotamers of $(R)$-[$^2H_1$, $^2H_2$, $^2H_3$]-neopentane would be too small for ROA to be measurable except in the 720 to 950 cm$^{-1}$ and the 1,150 to 1,340 cm$^{-1}$ spectral regions[9]. Even for these two spectral regions, the size of the computed $\varDelta$ values is only a few times $10^{-5}$ in backscattering, with even smaller values for other scattering geometries. This made the backscattering geometry the one most likely to allow us to confirm spectroscopically the chirality of $(R)$-[$^2H_1$, $^2H_2$, $^2H_3$]-neopentane.

The physical properties of the compound—its boiling point is expected to be 9.5 °C, the same as for neopentane and perdeuterated neopentane—the long measurement times needed to recover ROA for small Raman bands with tiny $\varDelta$ values, and the small amount of substance available, made it necessary to perform the measurements in a sealed capillary. Backscattering requires us to orient a capillary's axis perpendicularly to the direction of the exciting laser beam[5]. This arrangement is more 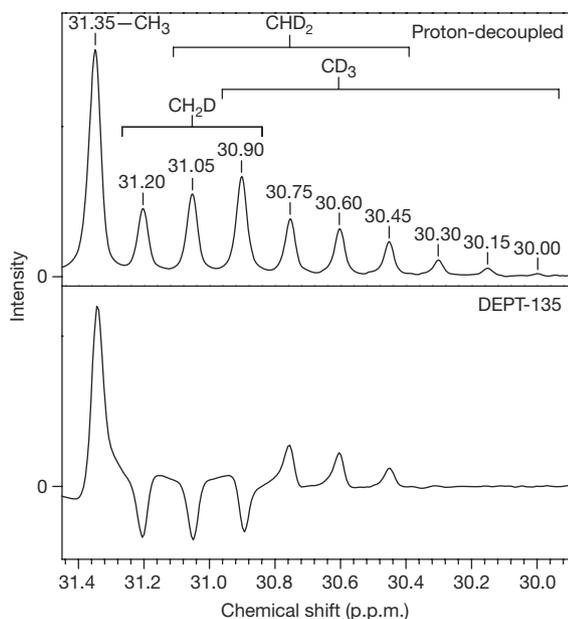prone to spurious signals than the use of cells with flat windows. In our scattered circular polarization experiment, in which the amount of right and left circularly polarized scattered light is analysed, the optical properties of the sample cell matter least for Raman bands for which the degree of circularity[15] is zero or slightly positive, which is the case for the 720 to 950 cm$^{-1}$ and the 1,150 to 1,340 cm$^{-1}$ region (see Supplementary Information).

The scattered circular polarization ROA instrument[16] (see Supplementary Information) used in this work is based on the design of an earlier one[4]. A dual-arm light-collection arrangement with fibre optics permits the simultaneous analysis of right and left circularly polarized scattered light, and an error-correction scheme[5] reduces deterministic spurious signals by creating the chiroptical properties of the enantiomeric sample, through optical means, from the sample physically present. Subtracting the signals makes the technique equivalent to recovering optical activity from a measurement of both enantiomers. Linearly polarized components of light are scrambled throughout all optical paths.
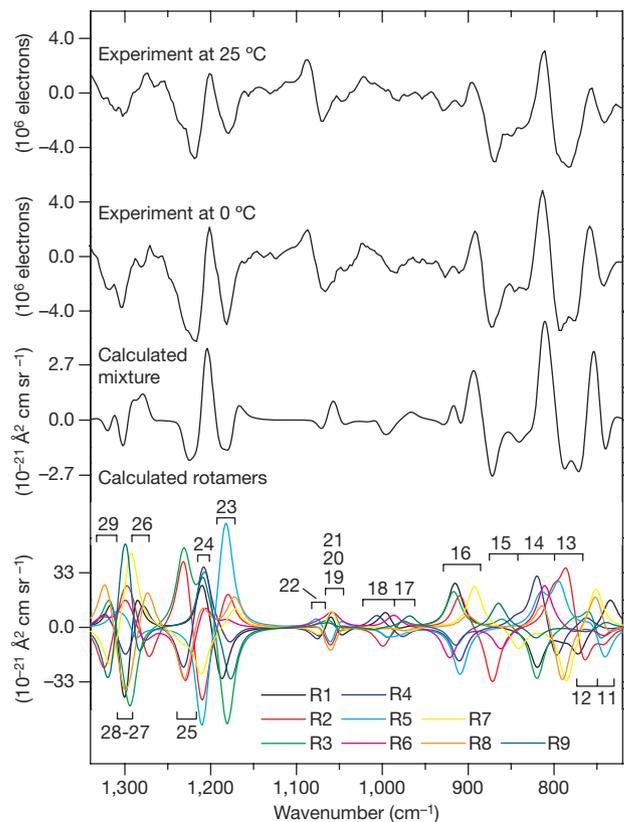


**Figure 3 | ROA spectra of $(R)$-[$^2H_1$, $^2H_2$, $^2H_3$]-neopentane.** The upper two traces show measured ROA spectra with temperatures as indicated. The lower traces show computed individual ROA spectra for the nine rotamers R1 to R9 (colours as indicated) and the average ROA spectrum for the mixture of all rotamers. The number of electrons is per column on the charge-coupled device (CCD) detector, which corresponds to 2.4 cm$^{-1}$. The numbers in the computed spectra refer to the vibrations of the nine rotamers. The measurement parameters are: exposure time, 40 h; laser power at sample, 300 mW; exciting wavelength, 532 nm; resolution, 7 cm$^{-1}$; sample size, 5.1 mg. The experimental spectra were smoothed by a third-order seven-point Savitzky–Golay procedure. The computational parameters are: density functional theory with the B3LYP functional and the augmented correlation consistent polarized valence double zeta (aug-cc-pVDZ) basis set for geometry and vibrations as implemented in Gaussian 03 (ref. 28); time-dependent Hartree-Fock with the aug-cc-pVDZ basis set for electronic tensors as implemented in the molecular electronic structure program DALTON (release 1.1 in 2000; http://www.kjemi.uio.no/software/dalton/dalton.html). The computed wavenumbers were multiplied by a scaling factor of 0.9875 to account for anharmonicity. See text for band shape parameters.



**Figure 2 | $^{13}$C-NMR characterization of the quaternary centre.** Upper panel, broadband proton-decoupled spectrum. Lower panel, DEPT-135 spectrum.

The ROA and Raman spectra for the mixture of the rotamers are shown in Figs 3 and 4, together with those computed for individual rotamers. This makes it clear that the computed bands do not correspond to individual vibrational modes. Rather, each band is the result of the superposition of the ROA or Raman intensities of many modes of different conformers, a situation which is not uncommon in vibrational optical activity.

That the computed and measured ROA data agree to the extent they do is impressive. The ROA of individual rotamers, often of opposite sign, exceeds the ROA of the mixture by more than an order of magnitude. The relative size, and the relative position, calculated for the ROA bands of different rotamers, must therefore be of a far higher precision than has up to now been judged attainable. The dependence of the theoretical spectra on computational details was carefully checked. We have attributed the stability we found to the $T_d$ site symmetry of the molecule, the close to identical electron distribution of the rotamers, and the observation that normal coordinates of energetically close vibrational modes of different rotamers decompose similarly into valence coordinates.

The choice of band shapes for rendering the theoretical spectra is important in a comparison with measured ones[9]. We assumed the lineshape function of the instrument to be gaussian with a full-width at half-maximum height (FWHM) of 7 cm$^{-1}$. The lineshape of the instrument was convoluted with lorentzian curves of 10 cm$^{-1}$ and 18 cm$^{-1}$ FWHM for the computed isotropic and anisotropic intensities, respectively. These values, which must be considered averages for different bands, gave the best agreement with the measured data at hand, including the Raman spectra of ordinary and of perdeuterated neopentane. For these compounds the complication of the presence of different conformers does not exist.

In the limited temperature range accessible to our instrument, the anisotropic lineshape was found to vary more than the isotropic one with the sample temperature. The visible sharpening of the Raman

spectrum in Fig. 4 upon lowering the temperature from 25 to 0 °C can be attributed to the narrowing of the anisotropic band shape of individual rotamers. Similarly, in Fig. 3, the ROA spectrum measured at 0 °C has a higher amplitude than the spectrum measured at 25 °C and appears to be, to the extent that noise permits such a conclusion, more structured. We note that ROA measured in backscattering is purely anisotropic.

The internal rotational barrier of the methyl groups of neopentane has been the subject of much interest. Thermodynamic data[17], the frequency of the methyl torsional mode[18,19], and cold neutron scattering[20,21] yield values between 18 and 21 kJ per mole. This amounts to about seven times the value of $kT$ at room temperature. The molecule's different rotamers therefore do not convert rapidly into each other. The amplitude of the hindered rotational motion of the methyl groups was estimated from model potentials to be about 15° at room temperature[22]. The C–C stretching force constant was found to depend on the torsional angle[23]. The stronger variation with temperature of the anisotropic band shape than of the isotropic one makes it unlikely that this is the main cause for the changes in the Raman and ROA spectra we observe. More probably, these changes are due to the temperature dependence of the librational motions of the whole $(R)$-[$^2$H$_1$, $^2$H$_2$, $^2$H$_3$]-neopentane molecules in the liquid phase. The substantial size of the changes, despite the modest measured temperature range of only 25 °C, is put into perspective by the fact that it is equivalent to the span between the melting and boiling point of neopentane at 1 bar. From the temperature dependence of the entropy we also know that onset of molecular reorientation occurs at −133 °C, at the passage to a face-centred cubic crystal structure[21].

The vibrations in the 720 to 950 cm$^{-1}$ region are dominated by the rocking motions of whole methyl groups[9]. In the 1,150 to 1,350 cm$^{-1}$ region, C–C bond stretching and the deformation of the methyl groups becomes important. In each of the two spectral regions, the distribution of vibrational energy shifts from the deuterium to the hydrogen nuclei with increasing frequency.

The synthesis of $(R)$-[$^2$H$_1$, $^2$H$_2$, $^2$H$_3$]-neopentane, the spectroscopic proof of its chiral nature, and the actual determination of the absolute configuration of this chemically inert, pure hydrocarbon molecule with $T_d$ site symmetry, all extend the scope of chiral chemistry and of vibrational optical activity. Although the measurement of optical activity of molecules chiral by isotope substitution has been accomplished in the past, in the ultraviolet[24], by Raman spectroscopy[25,26], and in the infrared[27], none of the molecules measured presented the challenges faced here: a highly symmetric electron distribution, absence of an electronic chromophore, and the presence of multiple, equally weighted conformers with mutually cancelling optical activity. There should remain few, if any, chiral systems the absolute configuration of which is not now spectroscopically accessible, either by anomalous X-ray scattering, by vibrational optical activity, or, under favourable circumstances, by the classical chiroptical methods of electronic rotatory dispersion and circular dichroism.

The reason that vibrational optical activity is so demonstrably more powerful than the methods mentioned above is that any chiral molecule must comprise at least four nuclei in a non-planar arrangement, and it will thus have a minimum of six vibrational modes reflecting its absolute configuration. Their shape is not the only, but is the decisive aspect in the computation of vibrational optical activity. Once a molecule's force field is known, calculating vibrational modes becomes largely a problem of classical mechanics. The calculation of a force field precise enough for determining the absolute configuration of a molecule like $(R)$-[$^2$H$_1$, $^2$H$_2$, $^2$H$_3$]-neopentane can be done with little expense, as we have demonstrated here.



**Figure 4 | Raman spectra of $(R)$-[$^2$H$_1$, $^2$H$_2$, $^2$H$_3$]-neopentane.** The upper two traces show measured Raman spectra with temperature as indicated. The lower traces show computed individual Raman spectra for the nine rotamers R1 to R9 (colours as indicated) and the average Raman spectrum for the mixture of all rotamers. Experimental and computational parameters are as in Fig. 3.

## METHODS

For the Raman and ROA measurements, Minicaps of length 30 mm with an inner diameter of 1.3 mm and a wall thickness of 0.2 mm were used. A Minicap was fused at one end, evacuated, cooled with liquid nitrogen, and
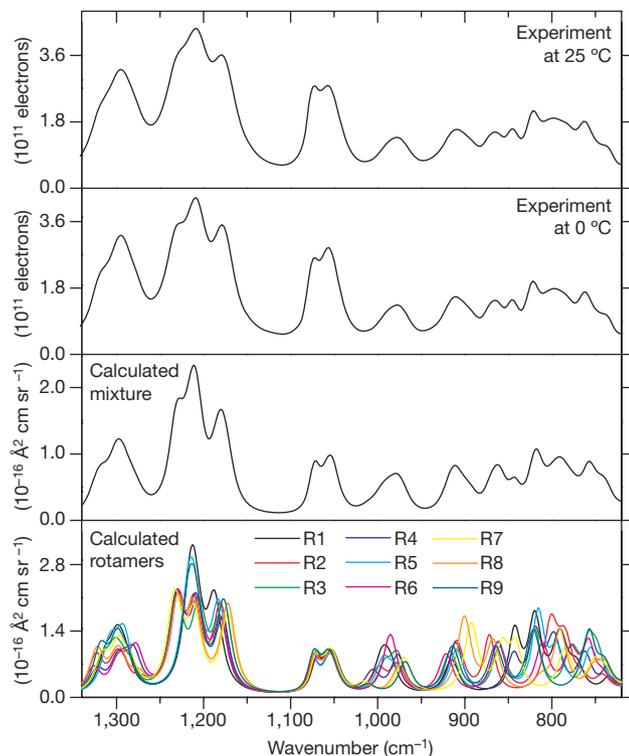
5.1 mg (8.5 µl) of $(R)$-[$^2$H$_1$, $^2$H$_2$, $^2$H$_3$]-neopentane condensed into it, directly from the Schlenk tube in which the compound had been synthesized. Fusion of the other end yielded a hermetically sealed sample of $(R)$-[$^2$H$_1$, $^2$H$_2$, $^2$H$_3$]-neopentane, slightly pressurized at room temperature, on which measurements could be performed. The laser power was kept at a relatively low 300 mW at the sample to avoid warming the capillary and distilling neopentane from the scattering zone to cooler parts during the long measurement sessions, typically lasting about 40 h. Measurements below room temperature were done while blowing dried cold air into a cage surrounding the capillary. Neopentane freezes at $-16.5\,^\circ$C and the perdeuterated form at $-18\,^\circ$C, which suggests a similar lower temperature limit for performing ROA measurements on liquid $(R)$-[$^2$H$_1$, $^2$H$_2$, $^2$H$_3$]-neopentane. In practice, we had to limit the lowest temperature to $0\,^\circ$C to avoid condensation on the light-collection optics of the instrument.

1. Bijvoet, J. M., Peerdeman, A. F. & van Bommel, A. J. Determination of the absolute configuration of optically active compounds by means of X-rays. *Nature* **168**, 271–272 (1951).
2. Barron, L. D., Bogaard, M. P. & Buckingham, A. D. Raman scattering of circularly polarized light by optically active molecules. *J. Am. Chem. Soc.* **95**, 603–605 (1973).
3. Holzwarth, G., Hsu, E. C., Mosher, H. S., Faulkaner, T. R. & Moscowitz, A. Infrared circular dichroism of carbon-hydrogen and carbon-deuterium stretching modes. Observations. *J. Am. Chem. Soc.* **96**, 251–252 (1974).
4. Hug, W. & Hangartner, G. A novel high-throughput Raman spectrometer for polarization difference measurements. *J. Raman Spectrosc.* **30**, 841–852 (1999).
5. Hug, W. Virtual enantiomers as the solution of optical activity's deterministic offset problem. *Appl. Spectrosc.* **57**, 1–13 (2003).
6. Helgaker, T., Ruud, K., Bak, K. L., Joergensen, P. & Olsen, J. Vibrational Raman optical activity calculations using London atomic orbitals. *Faraday Discuss.* **99**, 165–180 (1994).
7. Ruud, K., Helgaker, T. & Bouř, P. Gauge-origin independent density-functional theory calculations of vibrational Raman optical activity. *J. Phys. Chem. A* **106**, 7448–7455 (2002).
8. Zuber, G. & Hug, W. Rarefied basis sets for the calculation of optical tensors. 1. The importance of gradients on hydrogen atoms for the Raman scattering tensor. *J. Phys. Chem.* **108**, 2108–2118 (2004).
9. Hug, W. & Haesler, J. Is the vibrational optical activity of $(R)$-[$^2$H$_1$, $^2$H$_2$, $^2$H$_3$]-neopentane measurable? *Int. J. Quantum Chem.* **104**, 695–715 (2005).
10. Costante, J., Hecht, L., Polavarapu, P. L., Collet, A. & Barron, L. D. Absolute configuration of bromochlorofluoromethane from experimental and *ab initio* theoretical vibrational Raman optical activity. *Angew. Chem. Int. Edn Engl.* **36**, 885–887 (1997).
11. Crassous, J. & Collet, A. The bromochlorofluoromethane saga. *Enantiomer* **5**, 429–438 (2000).
12. Jiang, Z., Crassous, J. & Schurig, V. Gas-chromatographic separation of tri(hetero)halogenomethane enantiomers. *Chirality* **17**, 488–493 (2005).
13. Abe, T., Suzuki, T., Sekiguchi, K., Hosokawa, S. & Kobayashi, S. Stereoselective construction of a quaternary carbon substituted with multifunctional groups: application to the concise synthesis of (+)-ethosuximide. *Tetrahedr. Lett.* **44**, 9303–9305 (2003).
14. Barron, L. D. *Molecular Light Scattering and Optical Activity* 162, Ch. 3 (Cambridge Univ. Press, Cambridge, 2004).
15. Long, D. A. *Raman Spectroscopy* 130 (McGraw-Hill, New York, 1977).
16. Haesler, J. *Construction of a New Forward and Backward Scattering Raman Optical Activity Spectrometer and Graphical Analysis of Measured and Calculated Spectra for $(R)$-[$^2$H$_1$, $^2$H$_2$, $^2$H$_3$]-neopentane.* PhD thesis (Univ. Fribourg, 2006).
17. Pitzer, K. S. & Kilpatrick, J. E. The entropies and related properties of branched paraffin hydrocarbons. *Chem. Rev.* **39**, 435–447 (1946).
18. Weiss, S. & Leroi, G. E. Infrared spectra and internal rotation in propane, isobutane, and neopentane. *Spectrochim. Acta A* **25**, 1759–1766 (1969).
19. Durig, J. R., Craven, S. M. & Bragin, J. Low-frequency modes in molecular crystals. VI. Methyl torsions and barriers to internal rotation of C(CH$_3$)$_4$, C(CD$_3$)$_4$, Si(CH$_3$)$_4$, Ge(CH$_3$)$_4$, and Sn(CH$_3$)$_4$. *J. Chem. Phys.* **52**, 2046–2052 (1970).
20. Rush, J. J. Cold-neutron study of hindered rotations in solid and liquid methylchloroform, neopentane, and ethane. *J. Chem. Phys.* **46**, 2285–2291 (1967).
21. Grant, D. M., Strong, K. A. & Brugger, R. M. Direct observation of methyl librations in neopentane. *Phys. Rev. Lett.* **20**, 983–986 (1968).
22. Petryk, M. W. P. & Henry, B. R. Through space coupling and fermi resonances in neopentane-d$_0$, -d$_6$, -d$_9$, and tetramethylsilane. *J. Phys. Chem.* **106**, 8599–8608 (2002).
23. Palmo, K., Mirkin, N. G. & Krimm, S. Spectroscopically determined force fields for macromolecules. 2. Saturated hydrocarbon chains. *J. Phys. Chem. A* **102**, 6448–6456 (1998).
24. Barth, G. & Djerassi, C. Circular dichroism of molecules with isotopically engendered chirality. *Tetrahedron* **37**, 4123–4142 (1981).
25. Barron, L. D. Raman optical activity due to isotopic substitution: [α-2H]benzyl alcohol. *J. Chem. Soc. Chem. Commun.* **9**, 305–306 (1977).
26. Hug, W. Instrumental and theoretical advances in Raman optical activity. In *Raman Spectroscopy, Linear and Nonlinear* (eds Lascombe, J. & Huong, P. V.) 3 (John Wiley & Sons, Chichester, 1982).
27. Polavarapu, P. L., Nafie, L. A., Benner, S. A. & Morton, T. H. Optical activity due to isotopic substitution. Vibrational circular dichroism and the absolute configurations of α-deuterated cyclohexanones. *J. Am. Chem. Soc.* **103**, 5349–5359 (1981).
28. Frisch, M. J. *et al. Gaussian 03* Revision C.02 (Gaussian Inc., Wallingford, Connecticut, 2004).